Comparative Modeling of Power Hardening Micro-scale Metallic Plates Based on Lower and Higher-Order Strain Gradient Plasticity Theories

Amer Darvishvand[1] · Asghar Zajkani[1]

Abstract

Present study investigates a comparative study of lower and higher-order strain gradient plasticity (SGP) theories involving the size-dependent micromechanically flexural behaviors of crystalline thin plates. The investigation includes the Mechanism-Based and the Chen–Wang SGP models established on the Taylor dislocation hardening by evoking the statistically stored dislocations and geometrically necessary dislocations. In addition, these models are conjugated with a multiple plastic work-hardening law proposed for the microstructural applications of the SGP. An analytical approach based on energy minimizing method is used for obtaining deflection values in terms of the length scale, exponent of the work-hardening and the tangential module. The obtained results indicate a meaningful dependence of the deflections to the length scale, plastic work hardening and other parameters as well.

Keywords Crystalline thin films · Strain gradient plasticity · Length scale · Bending · Micro-plate · MSG theory · Chen–Wang hardening law

1 Introduction

Small-scale deformable structures have found tremendous applications in instrumentation and biosensors, micro-/Nano-electromechanical systems, and the atomic force microscopes [1–4]. There are few micromechanical theories available for the plastic flexural modeling of crystalline thin plates. Although some delicate operations have now manipulated for extremely small cases with the advent of advanced instruments, exploring material behaviors being possible at these scales are of interest for engineering design [5]. On the other hand, metallic and glassy thin films have been paid more attentions to explore their perspective properties in past decades. Some experiments done for understanding mechanical behaviors of the materials displaying significant size effect [6]. Some of related reports were prepared for micro bending [5, 7, 8], indentation process [9], wire torsion [10, 11] and film bulge test [12], bucking of micro plate [13] and bucking of micro beam [14]. In the indentation test on

thin film, Huber [15] found that the yield stress increases by decreasing the film thickness. Another experimental work shows that for the plates with one or several holes exposed tension, decreasing the size of hole caused to enhancing the flow stress [16, 17].

Since classical plasticity do not possess the internal material length scale, micromechanical modeling through theories of the classical continuum mechanics would not be successful. Therefore, the large number of theories were developed in terms of strain gradient elasticity (SGE) and SGP frameworks to solve the size-dependent structural problems. From primary research endeavors such as the work reported in [18], it is found that making a connection between the internal length scale and micro-structure may be provided through a multiplication term to high-order of the strain gradient terms. Actually, in the equations of gradient framework, the order gradient of necessary parameter with related coefficients can represent the material size-effect in such a way that two types of non-local continuum theories can take potentially opportunity to be developed. We strictly offer references of [5, 13] to review an encompassing literature about different types of the SGP theories. Here, due to diversity of the length scale-dependent continuum theories, we only draw reader's attentions to the phenomenological types extended on the J2 plasticity, and other continuum models derived from crystal

✉ Asghar Zajkani
zajkani@eng.ikiu.ac.ir

1   Department of Mechanical Engineering, Faculty of Engineering, Imam Khomeini International University, Qazvin 34149-16818, Iran

plasticity approaches such as [19–21] are not reviewed. Generally, there are two categories of SGP known as low-order and higher-order theories. In the lower-order SGP, the plastic modulus for a work hardening phenomenon is only modified by incorporating the plastic strain-gradients [22]. Therefore, the forms of boundary conditions and surface traction remain as the same of traditional models.

A Taylor based nonlocal theory was introduced by Gao and et al. [23, 24] named as Mechanism-based strain gradient (MSG) plasticity. This theory is divided in two main branches in the micro and mesoscales. At first, flow strength is suitably rearranged to accounting for simultaneously GND and SSD, without incorporating high order stresses. At second, the models are somewhat large to conjoin the gradient of strain fields to notion of the GND and to construct a constitutive model based on the Taylor-dislocation hypotheses. Recently, Darvishvand and Zajkani [14] introduced a size-dependent plastic buckling behavior of micro-beams by using the conventional mechanism-based strain gradient (CMSG) plasticity that were introduced firstly by Huang et al. [25]. They also analyzed permanent flexural deflection of MEMS actuators established on the CMSG plasticity [5]. Chen and Wang [26] introduced a new hardening law which is originated from general framework of couple stress theory in SGP based on the J2 deformation theory. Here, we abbreviate it by CWSGP. The expected efficiency of this model is dependent on proper adopting boundary conditions of the problem.

By developing the principle of the virtual work, the higher-order SGP are conducted to conjugate higher order stresses with the plastic strain gradients by involving extra boundary conditions and traction to be interfered in the balance law. In the work conducted by [27], a considerable explanation of the model was presented to apply yield condition through accounting for both second and fourth-order gradients for the equivalent plastic strain rate. Actually, they are utilized instead of conventional infinitesimal elasticity and the classical flow rule. By using the rotation gradients and couple stress concepts, a physical-based descriptions of the SGP introduced by [28–30]. Gudmundson [31] generalized the Fleck and Hutchinson (FH) model [29, 30] for isotropic materials in such a way that the flow direction becomes collinear with the sum of the deviatoric Cauchy stress tensor and the divergence of moment stresses (or higher order stresses) associated with the plastic strain gradient.

On the other hands, some elasto-plastic analyses have been found in [32–36]. Mao [37] investigated the influence of SGP on the flexural response of micro-beam. In addition, Chen and Feng [33] and Vakil and Zajkani [8] analyzed the bending responses of the cantilevered micro beams using the CWSGP theory. Vakil and Zajkani [8] produced a micromechanically motivated CWSGP model by implementing an intermediate

mixture TTO law to define ductile-like plastic behavior of Titanium-boride/titanium functionally graded crystalline materials. Also, the elastoplastic behaviors of the microbeams were proposed based on the couple stress (CS) by [38] as well as the MSG theories by [39]. Recently, the CWSGP is further developed to consider the damage effect induced by deformation. In order to give readers a comprehensive understanding of CWSGP, the authors suggest reviewing the proper references [40–42] in this area.

On the base of author's surveying, there are not valuable theoretical studies for the plastic responses of the microfilms in such a way that are modeled among the microplate kinematic frameworks. On a contrary, there are some to extend a lot of work about elastic behaviors of micro scale structures based on the strain gradient elasticity. In this study, obtained results of the plastic bending of the microplates will be compared by two lower and higher-order SGP. Therefore, the MSG theory will be used for the highest order and the Chen–Wang model for the lower-order theories of the SGP. In addition, the effect of the elastic foundation is investigated individually.

2 Theoretical Framework

Corresponding to sizes of the plate and films, we can categorize like to Fig. 1.

2.1 Structural Kinematics

The plastic bending of simply-support microplate will be studied based on both MSG and Chen–Wang (CW) theories. The Kirchhoff kinematics is selected to define displacement fields of the plate at first

$$u_x = -z\frac{\partial w(x,y)}{\partial x}, \quad u_y = -z\frac{\partial w(x,y)}{\partial y}, \quad u_z = w(x,y) \tag{1}$$
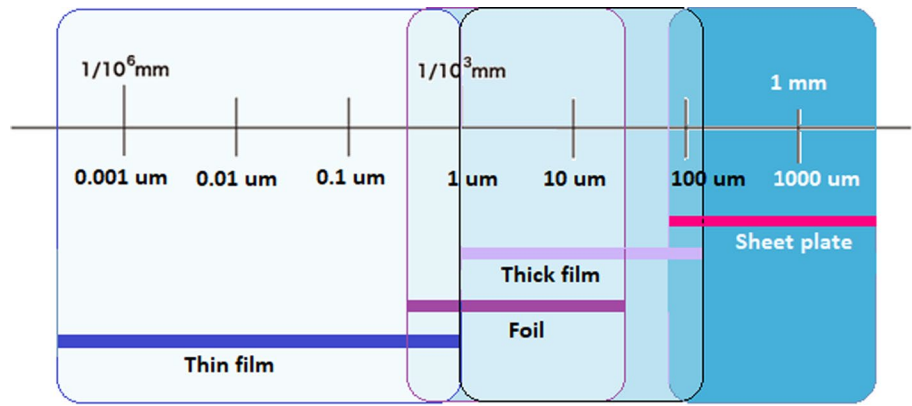
So, components of linear strain can be obtained as

$$\varepsilon_x = -z\frac{\partial^2 w}{\partial x^2}, \quad \varepsilon_y = -z\frac{\partial^2 w}{\partial y^2}, \quad \varepsilon_{xy} = -z\frac{\partial^2 w}{\partial y^2}$$

$$\varepsilon_z = \varepsilon_{yz} = \varepsilon_{zx} = 0 \tag{2}$$

Moreover, the deviatoric strains are evaluated in the following forms:

$$\varepsilon'_{ij} = \varepsilon_{ij} - \frac{\varepsilon_{mm}\delta_{ij}}{3}$$

$$\varepsilon'_x = \frac{z}{3}\left(\frac{\partial^2 w}{\partial y^2} - 2\frac{\partial^2 w}{\partial x^2}\right), \quad \varepsilon'_y = \frac{z}{3}\left(\frac{\partial^2 w}{\partial x^2} - 2\frac{\partial^2 w}{\partial y^2}\right)$$

$$\varepsilon'_z = \frac{z}{3}\left(\frac{\partial^2 w}{\partial x^2} + \frac{\partial^2 w}{\partial y^2}\right), \quad \varepsilon'_{xy} = -z\left(\frac{\partial^2 w}{\partial x\partial y}\right)$$

$$\varepsilon'_{xz} = \varepsilon'_{yz} = 0 \tag{3}$$

Fig. 1 Categorization of the films

The effective plastic strain and stress can be equivalently calculated by regarding the known Von-Mises criterion:

$$\bar{\varepsilon} = \sqrt{\frac{2}{3}\varepsilon'_{ij}\varepsilon'_{ij}} \tag{4}$$

$$\bar{\sigma} = \sqrt{\frac{2}{3}\sigma'_{ij}\sigma'_{ij}} \tag{5}$$

By substituting relation (3) into (4), the effective strain can be produced

$$\bar{\varepsilon} = \frac{2}{3}z\sqrt{A} \tag{6}$$

$$A = \left(\frac{\partial^2 w}{\partial x^2}\right)^2 + \left(\frac{\partial^2 w}{\partial y^2}\right)^2 - \left(\frac{\partial^2 w}{\partial x^2}\right)\left(\frac{\partial^2 w}{\partial y^2}\right) + \frac{3}{2}\left(\frac{\partial^2 w}{\partial x \partial y}\right)^2 \tag{7}$$

A schematic microplate, which is exposed under distributed transverse loading and is resting on elastic foundation, has been illustrated in Fig. 2.

Corresponding to the Fig. 2, the work due to the loading is obtained as [43]:

$$W_{external} = \int_0^b \int_0^a q(x,y)w\,dx\,dy \tag{8}$$

In addition, we apply a substrate layer that surrounds the main sheet. The surrounding elastic medium is generally modeled as Winkler-type elastic medium. The Winkler-type elastic foundation is approximated as a series of closely spaced, mutually independent, vertical linear elastic springs. The elastic medium modulus is represented by stiffness of the springs. However, this model is considered as a crude approximation of the true mechanical behavior of the elastic material. This is due to inability of the model to take into account the continuity or cohesion of the medium. The interaction between the springs is not taken into account in Winkler-type elastic
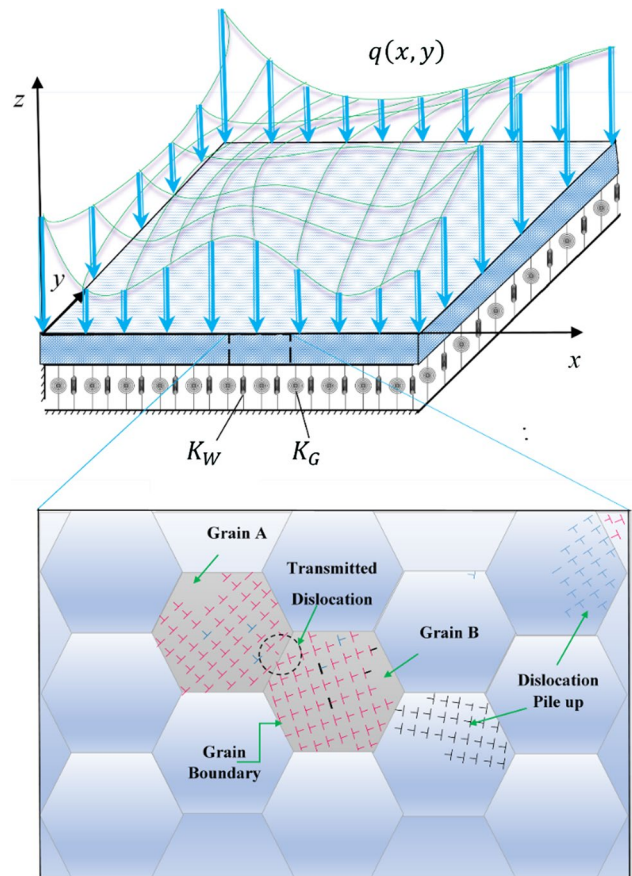

Fig. 2 The microplate over the elastic medium under transvers bending load

medium. A more realistic and generalized representation of the elastic medium can be accomplished by the way of a two-parameter elastic medium model. Thus, two-parameter elastic medium model is preferred. One such physical elastic medium model is the Pasternak-type elastic medium model. The first parameter of Pasternak elastic medium model represents the normal pressure while second parameter accounts for the transverse shear stress due to interaction of shear deformation of the surrounding

elastic medium. Pasternak-type model is physically realistic representation of the elastic medium. Further, it is a mathematically simple model for analyzing the surrounding elastic medium. In this model, existence of shear interaction among the spring elements is accomplished by connecting the ends of the springs to a beam or plate that only undergoes transverse shear deformation. The load–deflection relationship is obtained by considering the vertical equilibrium of a shear layer. Successful use of the Pasternak-type elastic medium model for simulating the interaction of the surrounding elastic medium were reported in [44, 45] for bending and vibration analyses of microplates and in [46] for nanovibration of multi-layered graphene sheets. Complete review of Winkler's foundation and its profound influence on adhesion and soft matter applications has been introduced in [47]. For example, applicability of Winkler's foundations has been described by using morphology of tree frog toe pads showing a microstructure that consists of an epidermis with hexagonal epithelial cells. In another work, a functionalized graphene FET enzymatic glucose biosensor was stabilized through silk/GOx film and silk substrate, which can be modeled by the Pasternak medium [48].

It is modeled through two linear elastic mediums of the Winkler and Pasternak formulations as follows (as shown in Fig. 2):

$$F_{\text{Elastic medium}} = -K_w w + K_G \left(\frac{\partial^2 w}{\partial x^2} + \frac{\partial^2 w}{\partial y^2} \right) \tag{9}$$

where K_w indicates the Winkler spring and K_G denotes the Pasternak shear modules. In addition, the work of the elastic foundation is considered as

$$W_{\text{Elastic medium}} = \int_0^b \int_0^a \left(-K_w w + K_G \left(\frac{\partial^2 w}{\partial x^2} + \frac{\partial^2 w}{\partial y^2} \right) \right) w dx dy \tag{10}$$

Accordingly, total work can be calculated as

$$W_{\text{totoal}} = W_{\text{external}} + W_{\text{Elastic medium}}$$
$$= \int_0^b \int_0^a \left(-q(x,y) - K_w w + K_G \left(\frac{\partial^2 w}{\partial x^2} + \frac{\partial^2 w}{\partial y^2} \right) \right) w dx dy \tag{11}$$

3 Mechanism-Based Strain Gradient (MSG) Plasticity

The Taylor's dislocation-based hardening model was proposed by Gao and Nix [18] through generalization of the Peach–Koehler force for a critical definition of resolved shear stress among distance between an interacting dominant moving dislocation pair (L_0). The model was named as the MSG expressed in terms of the SSD and GND, which these densities are denoted by ρ_S and ρ_G, respectively (see the work produced by Darvishvand and Zajkani [13])

$$\tau = \alpha_0 \mu b \sqrt{\rho_T} = \alpha_0 \mu b \sqrt{\rho_S + \rho_G} \tag{12}$$

where ρ_T implies on the total dislocation density and $0.1 \leq \alpha_0 \leq 0.5$ is a material constant. Also, μ and b indicate the shear modulus and Burgers vector, respectively. In addition, the density of ρ_G can be evaluated versus effective plastic strain gradient η and Nye-factor $\bar{r}$ [39] as

$$\rho_G = \bar{r} \frac{\eta}{b} \tag{13}$$

Taylor factor M can relate flow stress σ_{flow} versus the shear flow stress

$$\sigma_{flow} = M\tau = M\alpha\mu b \sqrt{\rho_s + \bar{r}\frac{\eta}{b}} \tag{14}$$

For FCC metals $M = 3.06$ [49, 50]. In the absence of the strain gradient, the above relation descends to the classical plasticity as follows

$$\sigma_{flow} = M\alpha\mu b \sqrt{\rho_s} = \sigma_Y f(\bar{\varepsilon}) \tag{15}$$

where $\sigma_Y f(\bar{\varepsilon})$ provides the stress–strain curve in uniaxial tension (σ_Y denotes initial yield stress, and f represents a non-dimensional function of the effective plastic strain $\bar{\varepsilon}$). By substitution of above relations, we have [13]

$$\sigma_{flow} = \sqrt{[\sigma_Y f(\bar{\varepsilon})]^2 + M^2 \bar{r} \alpha_0^2 \mu^2 b \eta^p} = \sigma_Y \sqrt{f^2(\bar{\varepsilon}) + l\eta} \tag{16}$$

where l shows material length scale

$$l = M^2 \bar{r} \alpha_0^2 \left(\frac{\mu}{\sigma_Y} \right)^2 b = 18\alpha_0^2 \left(\frac{\mu}{\sigma_Y} \right)^2 b \tag{17}$$

The following simple power law is proposed for describing the isotropic hardening behavior:

$$f(\bar{\varepsilon}) = \bar{\varepsilon}^N \tag{18}$$

where N indicates the exponent the plastic work hardening. Therefore,

$$\sigma_{flow} = \sigma_Y \sqrt{\bar{\varepsilon}^{2N} + l\eta} \tag{19}$$

So, proportional to the displacement field attributed in Eq. (1), we can drive the strain gradients $(\eta_{ijk} = u_{k,ij})$:

$$\eta_{111} = -z\frac{\partial^3 w}{\partial x^3}, \quad \eta_{222} = -z\frac{\partial^3 w}{\partial y^3}$$

$$\eta_{121} = \eta_{211} = \eta_{112} = -z\frac{\partial^3 w}{\partial x^2 \partial y}$$

$$\eta_{221} = \eta_{122} = \eta_{212} = -z\frac{\partial^3 w}{\partial x \partial y^2}$$

$$\eta_{131} = \eta_{311} = -\eta_{113} = -\frac{\partial^2 w}{\partial x^2}$$

$$\eta_{232} = \eta_{322} = -\eta_{223} = -\frac{\partial^2 w}{\partial y^2}$$

$$\eta_{231} = \eta_{321} = \eta_{132} = \eta_{312} = -\eta_{123} = -\eta_{213} = -\frac{\partial^2 w}{\partial x \partial y}$$

$$\eta_{331} = \eta_{332} = \eta_{133} = \eta_{233} = \eta_{313} = \eta_{323} = \eta_{333} = 0$$

(20)

According to derivations reported by Vakil and Zajkani [8], the deviatoric part of the strain gradient is defined as

$$\eta'_{ijk} = \eta_{ijk} - \frac{1}{4}\left(\delta_{ik}\eta_{jpp} - \delta_{jk}\eta_{ipp}\right) \tag{21}$$

Combining above relations leads to extract components of the deviatoric strain gradients as

$$\eta'_{121} = \eta'_{211} = \frac{z}{4}\left(-3\frac{\partial^3 w}{\partial x^2 \partial y} + \frac{\partial^3 w}{\partial y^3}\right)$$

$$\eta'_{131} = \eta'_{311} = \frac{1}{4}\left(-3\frac{\partial^2 w}{\partial x^2} + \frac{\partial^2 w}{\partial y^2}\right)$$

$$\eta'_{122} = \eta'_{212} = \frac{z}{4}\left(-3\frac{\partial^3 w}{\partial x \partial y^2} + \frac{\partial^3 w}{\partial x^3}\right),$$

$$\eta'_{232} = \eta'_{322} = \frac{1}{4}\left(-3\frac{\partial^2 w}{\partial y^2} + \frac{\partial^2 w}{\partial x^2}\right)$$

$$\eta'_{133} = \eta'_{313} = \frac{z}{4}\left(\frac{\partial^3 w}{\partial x^3} + \frac{\partial^3 w}{\partial x \partial y^2}\right),$$

$$\eta'_{233} = \eta'_{323} = \frac{z}{4}\left(\frac{\partial^3 w}{\partial y^3} + \frac{\partial^3 w}{\partial x^2 \partial y}\right)$$

$$\eta'_{111} = \frac{z}{2}\left(-\frac{\partial^3 w}{\partial x^3} + \frac{\partial^3 w}{\partial x \partial y^2}\right), \quad \eta'_{222} = \frac{z}{2}\left(-\frac{\partial^3 w}{\partial y^3} + \frac{\partial^3 w}{\partial x^2 \partial y}\right)$$

$$\eta'_{333} = \frac{z}{2}\left(\frac{\partial^2 w}{\partial x^2} + \frac{\partial^2 w}{\partial y^2}\right), \quad \eta'_{331} = \eta'_{332} = 0$$

$$\eta'_{112} = -z\frac{\partial^3 w}{\partial x^2 \partial y}, \quad \eta'_{221} = -z\frac{\partial^3 w}{\partial x \partial y^2}$$

$$\eta'_{113} = \frac{\partial^2 w}{\partial x^2}, \quad \eta'_{223} = \frac{\partial^2 w}{\partial y^2}$$

$$\eta'_{231} = \eta'_{321} = \eta'_{132} = \eta'_{312} = -\eta'_{123} = -\eta'_{213} = -\frac{\partial^2 w}{\partial x \partial y}$$

(22)

In addition, the effective strain gradient becomes:

$$\eta = \sqrt{\frac{1}{4}\eta'_{ij}\eta'_{ij}} \tag{23}$$

Substituting elations (22) into Eq. (23) results

$$\eta = \frac{1}{2}\sqrt{\frac{z^2}{4}B + C} \tag{24}$$

where

$$B = 2\left(\frac{\partial^3 w}{\partial x^3} - \frac{\partial^3 w}{\partial x \partial y^2}\right)^2 + 2\left(\frac{\partial^3 w}{\partial y^3} - \frac{\partial^3 w}{\partial x^2 \partial y}\right)^2 + \left(\frac{\partial^2 w}{\partial x^2} + \frac{\partial^2 w}{\partial y^2}\right)^2 + 8\left(\left(\frac{\partial^3 w}{\partial x^2 \partial y}\right)^2 + \left(\frac{\partial^3 w}{\partial x \partial y^2}\right)^2\right)$$

(25)

$$C = \frac{1}{4}\left(3\frac{\partial^2 w}{\partial x^2} - \frac{\partial^2 w}{\partial y^2}\right)^2 + 2\left(\frac{\partial^2 w}{\partial y^2}\right)^2 + 6\left(\frac{\partial^2 w}{\partial x \partial y}\right)^2 \tag{26}$$

Using the Von-Mises yield surface in the deformation theory of the MSG plasticity gives

$$\sigma'_{ij} = \frac{2\varepsilon_{ij}}{3\bar{\varepsilon}}\sigma_{flow} = \frac{2\varepsilon_{ij}}{3\bar{\varepsilon}}\sigma_Y\sqrt{\bar{\varepsilon}^{2N} + l\eta} \tag{27}$$

According to the MSG plasticity as the same of scheme employed in references [13, 51], the stress tensor is evaluated by adding the deviatoric and hydrostatic parts

$$\sigma_{ij} = K\varepsilon_{kk}\delta_{ij} + \frac{2\varepsilon'_{ij}}{3\bar{\varepsilon}}\sigma_{flow} = K\varepsilon_{kk}\delta_{ij} + \frac{2\varepsilon'_{ij}}{3\bar{\varepsilon}}\sigma_Y\sqrt{\bar{\varepsilon}^{2N} + l\eta} \tag{28}$$

where K denotes the elastic bulk modulus vanishing at the plastic area. The components of the non-vanishing parts (deviatoric stresses) are expressed as

$$\sigma'_x = \frac{2\varepsilon_x}{3\bar{\varepsilon}}\sigma_Y\sqrt{\bar{\varepsilon}^{2N} + l\eta} = -\frac{2}{3\bar{\varepsilon}}z\frac{\partial^2 w}{\partial x^2}\sigma_Y\sqrt{\bar{\varepsilon}^{2N} + l\eta} \tag{29}$$

$$\sigma'_y = \frac{2\varepsilon_y}{3\bar{\varepsilon}}\sigma_Y\sqrt{\bar{\varepsilon}^{2N} + l\eta} = -\frac{2}{3\bar{\varepsilon}}z\frac{\partial^2 w}{\partial y^2}\sigma_Y\sqrt{\bar{\varepsilon}^{2N} + l\eta} \tag{30}$$

$$\sigma'_{xy} = \frac{2\varepsilon_{xy}}{3\bar{\varepsilon}}\sigma_Y\sqrt{\bar{\varepsilon}^{2N} + l\eta} = -\frac{2}{3\bar{\varepsilon}}z\frac{\partial^2 w}{\partial x \partial y}\sigma_Y\sqrt{\bar{\varepsilon}^{2N} + l\eta} \tag{31}$$

Consequently, the strain energy can be calculated by the following integral

$$U = \frac{1}{2}\iiint_v \sigma'_{ij}\varepsilon'_{ij}dv = \frac{1}{2}\int_{-\frac{h}{2}}^{\frac{h}{2}}\int_0^b\int_0^a (\sigma'_x\varepsilon'_x + \sigma'_y\varepsilon'_y + 2\sigma'_{xy}\varepsilon'_{xy})dxdydz$$

(32)

Now, by substituting the stress and strain values, we can evaluate

$$U = \frac{\sigma_Y}{3} \int\limits_0^h \int\limits_0^b \int\limits_0^a \left(z\sqrt{A}\sqrt{\left(\frac{2}{3}z\sqrt{A}\right)^{2N} + \frac{l}{2}\sqrt{\frac{z^2}{4}B + C}} \right) dxdydz \tag{33}$$

Since the main nonlinearity source of the problem comes from the complicated radical part of the above equation, it can be converted to simple expression of power functions by means of short expansion of the twofold Taylor series:

$$\begin{aligned}
&z\sqrt{A}\sqrt{\left(\frac{2}{3}z\sqrt{A}\right)^{2N} + \frac{l}{2}\sqrt{\frac{z^2}{4}B + C}} \\
&= \frac{3}{16(1+l)^{\frac{3}{2}}} \left\{ l^2 \left[\left(\frac{4}{9}z^2A + 1\right)\left(\frac{B}{16}z^2 + \frac{C}{4} + 3\right) \right] \right. \\
&\quad - l\left[\frac{4}{9}z^2A\left((N-1)\left(\frac{B}{16}z^2 + \frac{C}{4}\right) - 5N - 7\right)\right. \\
&\quad \left. -(N+1)\left(\frac{B}{16}z^2 + \frac{C}{4}\right) + 5N - 7\right] + \frac{4}{9}z^2A(4N+4) - 4N + 4 \right\}
\end{aligned} \tag{34}$$

Thus, substituting the relation (34) into (33) and integrating at z-direction, results

$$U = \frac{\sigma_Y}{16(1+l)^{\frac{3}{2}}} \int\limits_0^b \int\limits_0^a \left(l^2\alpha + l\beta + \gamma\right) dxdy \tag{35}$$

where

$$\alpha = \frac{h^5}{2880}AB + \frac{h^3}{12}\left(\frac{1}{9}AC + \frac{4}{3}A + \frac{1}{16}B\right) + h\left(\frac{1}{4}C + 3\right)$$

$$\beta = -\frac{1}{144}\left\{ \frac{4h^5}{80}AB(N-1) + \frac{h^3}{12}[A((16C - 320)N - 16C - 448) - 9B(N+1)] \right.$$

$$\left. + h[(-36C + 720)N - 36C - 1008] \right\}$$

$$\gamma = \frac{16}{108}h^3A(N+1) - 4h(N+1)$$

(36)

Here, the total potential energy is used applied for the principle of minimizing as

$$\Pi = U - W_{\text{total}} \tag{37}$$

Therefore, the Eqs. (11) and (35) are combined in (37) to take the following energy functional:

$$\Pi = \frac{1}{2} \int\limits_0^b \int\limits_0^a \left(\frac{\sigma_Y(l^2\alpha + l\beta + \gamma)}{8(1+l)^{\frac{3}{2}}} \right.$$

$$\left. + w\left(q + K_w w - K_G\left(\frac{\partial^2 w}{\partial x^2} + \frac{\partial^2 w}{\partial y^2}\right)\right)\right) dxdy \tag{38}$$

4 The Chen–Wang (CW) Hardening Model

Upon the material dimension decreases to the micron level, a strong dependency of the material behavior on the size effect will be evidently revealed. The influence of length scale parameter on the SGP approach is enough effective to investigate drastic microstructural behaviors. However, the strain gradient theory proposed by Chen and Wang (CWSGP) is derived originally from a general couple stress framework [8], but it incorporates a hardening law by a new phenomenological way [26]. Since, the CWSGP is configured based on the J_2 deformation theory, it is excepted that sufficient boundary conditions should be adopted to generate satisfactory accuracy, as compared to available experiments by Fleck et al. [10] and Stolken and Evans [7].

According to primary definitions, the time derivative of the stress is defined as

$$\dot{\sigma} = \frac{3}{2}E_p\dot{\bar{\varepsilon}}\left(1 + \frac{l_{cw}\eta}{\bar{\varepsilon}}\right)^{1/2} \tag{39}$$

where E_p and l_{cw} are these plastic module and rotation gradient length scale. In this paper, it is assumed that the plastic module is constant. Because the variations of the plastic module caused be that it not be possible the analytical solution of the problem [26, 53]. The equivalent strain gradient used in the Chen–Wang theory is obtained as [8]

$$\eta = \sqrt{c_1\eta_{ijk}^{(1)}\eta_{ijk}^{(1)} + x_e^2} \tag{40}$$

The $\eta_{ijk}^{(1)}$ is the stretching strain gradient that is

$$\eta_{ijk}^{(1)} = \frac{1}{3}\eta_{ijk}^s - \frac{1}{5}\left[\delta_{ij}\eta_{kpp}^s - \delta_{jk}\eta_{ipp}^s + \delta_{ki}\eta_{jpp}^s\right] \tag{41}$$

η^s represents the symmetric part of η

$$\eta_{ijk}^s = \frac{1}{3}\left[\eta_{ijk} + \eta_{jki} + \eta_{kij}\right] \tag{42}$$

The Cartesian strain gradients are individually extracted proportional to the displacement fields

$$\eta_{111}^{(1)} = -\frac{1}{3}z\frac{\partial^3 w}{\partial x^3} + \frac{16}{15}z\frac{\partial^3 w}{\partial x \partial y^2}, \quad \eta_{123}^{(1)} = \frac{2}{3}\frac{\partial^2 w}{\partial x \partial y}$$

$$\eta_{112}^{(1)} = -\frac{5}{9}z\frac{\partial^3 w}{\partial x^2 \partial y} + \frac{2}{5}z\frac{\partial^3 w}{\partial y^3}, \quad \eta_{131}^{(1)} = \frac{1}{15}\frac{\partial^2 w}{\partial x^2}$$

$$\eta_{113}^{(1)} = \eta_{311}^{(1)} = -\frac{1}{45}\frac{\partial^2 w}{\partial x^2} + \frac{4}{45}\frac{\partial^2 w}{\partial y^2}, \quad \eta_{132}^{(1)} = \frac{4}{15}\frac{\partial^2 w}{\partial x \partial y}$$

$$\eta_{121}^{(1)} = -\frac{5}{9}z\frac{\partial^3 w}{\partial x^2 \partial y} + \frac{8}{45}z\frac{\partial^3 w}{\partial y^3}, \quad \eta_{223}^{(1)} = \eta_{232}^{(1)} = \frac{1}{5}\frac{\partial^2 w}{\partial y^2}$$

$$\eta_{122}^{(1)} = -\frac{5}{9}z\frac{\partial^3 w}{\partial x \partial y^2} + \frac{8}{45}z\frac{\partial^3 w}{\partial x^3}, \quad \eta_{312}^{(1)} = \eta_{321}^{(1)} = \frac{2}{5}\frac{\partial^2 w}{\partial x \partial y}$$

$$\eta_{133}^{(1)} = -\frac{1}{3}z\frac{\partial^3 w}{\partial x^3} + \frac{11}{15}z\frac{\partial^3 w}{\partial x \partial y^2}, \quad \eta_{332}^{(1)} = \frac{1}{45}\frac{\partial^2 w}{\partial y^2} + \frac{4}{45}\frac{\partial^2 w}{\partial x^2}$$

$$\eta_{211}^{(1)} = -\frac{46}{45}z\frac{\partial^3 w}{\partial x^2 \partial y} + \frac{8}{45}z\frac{\partial^3 w}{\partial y^3}, \quad \eta_{213}^{(1)} = \eta_{231}^{(1)} = \eta_{321}^{(1)} = \frac{2}{5}\frac{\partial^2 w}{\partial x \partial y}$$

$$\eta_{212}^{(1)} = -\frac{47}{45}z\frac{\partial^3 w}{\partial x \partial y^2} + \frac{2}{9}z\frac{\partial^3 w}{\partial x^3}, \quad \eta_{313}^{(1)} = \frac{37}{45}z\frac{\partial^3 w}{\partial x \partial y^2} + \frac{7}{45}z\frac{\partial^3 w}{\partial x^3}$$

$$\eta_{212}^{(1)} = -\frac{41}{45}z\frac{\partial^3 w}{\partial x \partial y^2} + \frac{4}{45}z\frac{\partial^3 w}{\partial x^3}, \quad \eta_{323}^{(1)} = \frac{7}{9}z\frac{\partial^3 w}{\partial x^2 \partial y} + \frac{11}{45}z\frac{\partial^3 w}{\partial y^3}$$

$$\eta_{222}^{(1)} = -\frac{16}{15}z\frac{\partial^3 w}{\partial x^2 \partial y} + \frac{1}{3}z\frac{\partial^3 w}{\partial y^3}, \quad \eta_{331}^{(1)} = \frac{7}{9}z\frac{\partial^3 w}{\partial x \partial y^2} + \frac{11}{45}z\frac{\partial^3 w}{\partial y^3}$$

$$\eta_{332}^{(1)} = \frac{11}{15}z\frac{\partial^3 w}{\partial x^2 \partial y} + \frac{1}{3}z\frac{\partial^3 w}{\partial y^3}, \quad \eta_{332}^{(1)} = \frac{1}{15}\left[\frac{\partial^2 w}{\partial x^2} + \frac{\partial^2 w}{\partial y^2}\right]$$

$$\eta_{233}^{(1)} = \eta_{332}^{(1)} = -\frac{11}{15}z\frac{\partial^3 w}{\partial x^2 \partial y} + \frac{1}{3}z\frac{\partial^3 w}{\partial y^3}$$

$$(43)$$

Also, it's constant the c_1 and

$$c_1 = \left(\frac{l_1}{l_{cw}}\right)^2 \tag{44}$$

Here, l_{cw} and l_1 define the intrinsic length scales devoted for the rotation and stretch gradients, respectively. Also, χ_e is defined as a second invariant of the curvature, as

$$\chi_e = \sqrt{\frac{2}{3}\chi_{ij}\chi_{ij}} \tag{45}$$

where

$$\chi_{ip} = \theta_{i,p} = \frac{1}{2}e_{ijk}u_{k,jp} = e_{ijk}\varepsilon_{kp,j} \tag{46}$$

Therefore, the equivalent curvature is calculated as

$$\chi_e = \sqrt{\frac{2}{3}\left[\left(\frac{\partial^2 w}{\partial x^2}\frac{\partial^2 w}{\partial y^2}\right)\frac{\partial^2 w}{\partial x \partial y}\right]} \tag{47}$$

The equivalent strain gradient in the CW theory is as

$$\eta = \left\{c_1\left[\frac{8}{9}z\frac{\partial^3 w}{\partial x^3} + \frac{4}{3}z\frac{\partial^3 w}{\partial y^3} + \frac{8}{9}z\frac{\partial^3 w}{\partial x \partial y^2}\right.\right.$$
$$+ \frac{38}{15}\frac{\partial^2 w}{\partial x \partial y} + \frac{53}{45}z\frac{\partial^3 w}{\partial x^2 \partial y} + \frac{4}{15}\frac{\partial^2 w}{\partial x^2}$$
$$\left.+ \frac{2}{3}\frac{\partial^2 w}{\partial y^2}\right]^2 + \left.\left[\left(\frac{\partial^2 w}{\partial x^2}\frac{\partial^2 w}{\partial y^2}\right)\frac{\partial^2 w}{\partial x \partial y}\right]^2\right\}^{1/2} \tag{48}$$

In addition, time integration of the relation (39) leads to obtain the following hardening law of the Chen–Wang (CW) theory:

$$\bar{\sigma} = \left(\sigma_Y + \frac{3}{2}E_p z\bar{\varepsilon}\right)\left(1 + \frac{l_{cw}\eta}{\bar{\varepsilon}}\right)^{1/2} \tag{49}$$

The CW model is categorized in the lower order SGP theories established over J_2 deformation theory. So

$$\sigma'_{ij} = \frac{2}{3}\frac{\bar{\sigma}}{\bar{\varepsilon}}\varepsilon'_{ij} \tag{50}$$

Therefore, we have

$$\sigma'_{ij} = \frac{2}{3}\left(\frac{\sigma_Y + \frac{3}{2}E_p z\bar{\varepsilon}}{\bar{\varepsilon}}\right)\left(1 + \frac{l_{cw}\eta}{\bar{\varepsilon}}\right)^{1/2}\varepsilon'_{ij} \tag{51}$$

By multiplying the stresses into corresponding deviatoric strains, we have

$$\sigma'_{ij}\varepsilon'_{ij} = \frac{2}{3}\left(\frac{\sigma_Y + \frac{3}{2}E_p z\bar{\varepsilon}}{\bar{\varepsilon}}\right)\left(1 + \frac{l_{cw}\eta}{\bar{\varepsilon}}\right)^{1/2}\left(\varepsilon'_{ij}\right)^2 \tag{52}$$

By replacing relations (52) into the strain energy and using relations (11), and (37), we have:

$$\Pi = \frac{1}{2}\int_0^h\int_0^b\int_0^a \Gamma\left\{5\left[\left(\frac{\partial^2 w}{\partial x^2}\right)^2 + \left(\frac{\partial^2 w}{\partial y^2}\right)^2\right] + 36\left(\frac{\partial^2 w}{\partial x \partial y}\right)^2\right.$$
$$\left.-8\left(\frac{\partial^2 w}{\partial x^2}\right)\left(\frac{\partial^2 w}{\partial y^2}\right)\right\}dzdxdy$$
$$+ \int_0^b\int_0^a + w\left(q(x,y) + K_w w - K_G\left(\frac{\partial^2 w}{\partial x^2} + \frac{\partial^2 w}{\partial y^2}\right)\right)dxdy \tag{53}$$

where

$$\Gamma = \left\{A_1 z^2 + \sqrt{B_1 z^4 + B_2 z^3 + B_3 z^2} + A_3 z^4 + A_5 z^3 + \sqrt{B_4 z^8 + B_5 z^7 + B_6 z^6}\right.$$
$$\left.+ \sqrt{B_7 z^6 + B_8 z^5 + B_9 z^5}\right\}^{1/2} \tag{54}$$

and

$$A_1 = \left(\frac{2}{24}\right)^2 \sigma_Y^2 \theta^{-1} A_3 = \left(\frac{2}{27}\right)^2 E_p^2 \left(\frac{3}{2}\right)$$

$$A_5 = 3\left(\frac{2}{27}\right)^2 E_p \theta^{-1/2} \sigma_Y$$

$$B_1 = c_1 \varphi^2 \left(\frac{2}{27}\right)^4 \sigma_Y^4 E_p \theta^{-3} l_{cw}^2$$

$$B_2 = c_1 \varphi^2 \left(\frac{2}{27}\right)^4 \sigma_Y^4 E_p \theta^{-3} l_{cw}^2$$

$$B_3 = (\vartheta + c_1 \psi^2)\left(\frac{2}{27}\right)^4 \sigma_Y^4 E_p \theta^{-3} l_{cw}^2$$

$$B_4 = c_1 \varphi^2 \left(\frac{2}{27}\right)^4 \left(\frac{3}{2}\right)^2 E_p^4 \theta^{-1} l_{cw}^2,$$

$$B_5 = 2c_1 \varphi\psi \left(\frac{2}{27}\right)^4 \left(\frac{3}{2}\right)^2 E_p^4 \theta^{-1} l_{cw}^2$$

$$B_6 = (\vartheta + c_1 \psi^2)\left(\frac{2}{27}\right)^4 \left(\frac{3}{2}\right)^2 E_p^4 \theta^{-1} l_{cw}^2$$

$$B_7 = c_1 \varphi^2 \left(\frac{2}{27}\right)^4 (3)^2 E_p^2 \sigma_Y^2 \theta^{-2} l_{cw}^2$$

$$B_8 = 2c_1 \varphi\psi \left(\frac{2}{27}\right)^4 (3)^2 E_p^2 \theta^{-2} \sigma_Y^2 l_{cw}^2$$

$$B_9 = (\vartheta + c_1 \psi^2)\left(\frac{2}{27}\right)^4 (3)^2 E_p^2 \theta^{-2} \sigma_Y^2 l_{cw}^2$$

(55)

Also,

$$\theta = \left(\frac{2}{27}\right)\left[\left(\frac{\partial^2 w}{\partial x^2}\right)^2 + \left(\frac{\partial^2 w}{\partial y^2}\right)^2\right]$$
$$- \left(\frac{16}{27}\right)\left(\frac{\partial^2 w}{\partial x^2}\right)^2\left(\frac{\partial^2 w}{\partial y^2}\right)^2 + \left(\frac{32}{3}\right)\left(\frac{\partial^2 w}{\partial x \partial y}\right)$$

$$\varphi = \left(\frac{2}{27}\right)\left(\frac{\partial^3 w}{\partial x^3}\right) + \left(\frac{4}{3}\right)\left(\frac{\partial^3 w}{\partial y^3}\right)$$
$$+ \left(\frac{8}{9}\right)\left(\frac{\partial^3 w}{\partial x \partial y^2}\right) + \left(\frac{53}{45}\right)\left(\frac{\partial^3 w}{\partial x^2 \partial y}\right)$$

$$\psi = \left(\frac{38}{15}\right)\left(\frac{\partial^2 w}{\partial x \partial y}\right) + \left(\frac{4}{15}\right)\left(\frac{\partial^2 w}{\partial x^2}\right)$$
$$+ \left(\frac{2}{3}\right)\left(\frac{\partial^2 w}{\partial y^2}\right)$$

$$\vartheta = \left(\frac{2}{3}\right)\left[\left(\frac{\partial^2 w}{\partial x^2}\right)\left(\frac{\partial^2 w}{\partial y^2}\right) - \left(\frac{\partial^2 w}{\partial x \partial y}\right)^2\right]^2$$
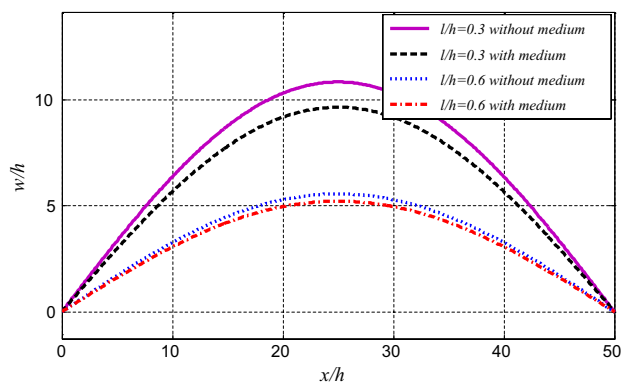
(56)

Fig. 3 The comparisons of dimensionless deflections of the plate; w/h for MSG theory versus the normalized variable length scales l/h concerning elastic medium
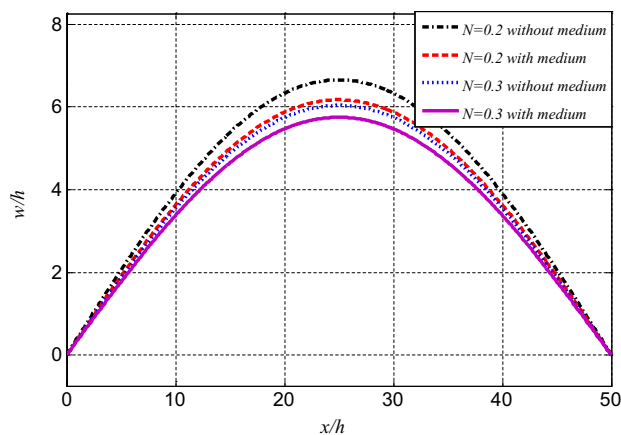

Fig. 4 The comparison of dimensionless deflection of the plate w/h for the MSG theory for two cases of plastic work hardening and the elastic medium effects
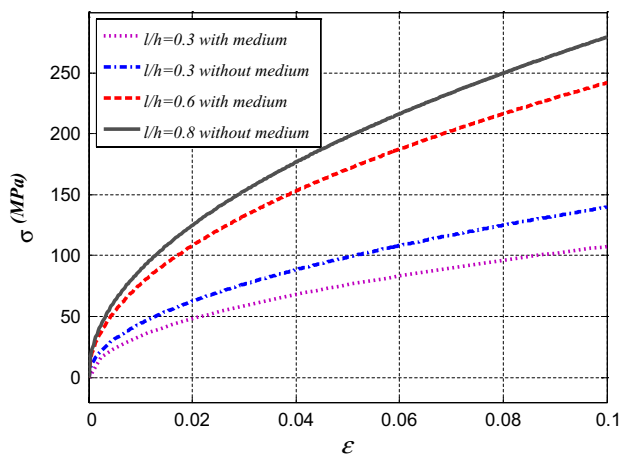

Fig. 5 The comparisons of the effective stress for the MSG theory in terms of the effective strain concerning the effect of elastic medium for two value of the normalized length scale l/h
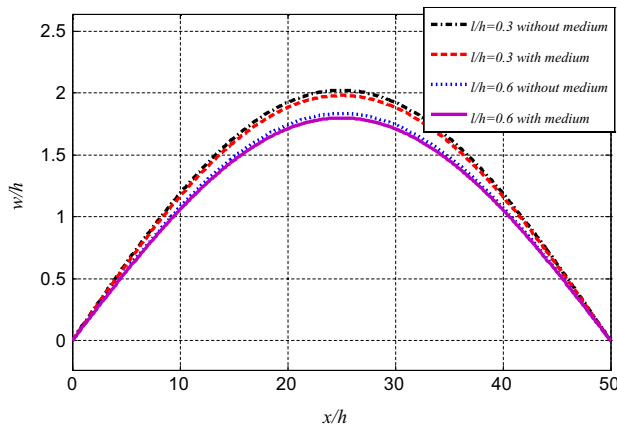
Fig. 6 The comparisons of dimensionless deflections for the CW theory versus the normalized variable length scale l/h concerning the effect of elastic medium
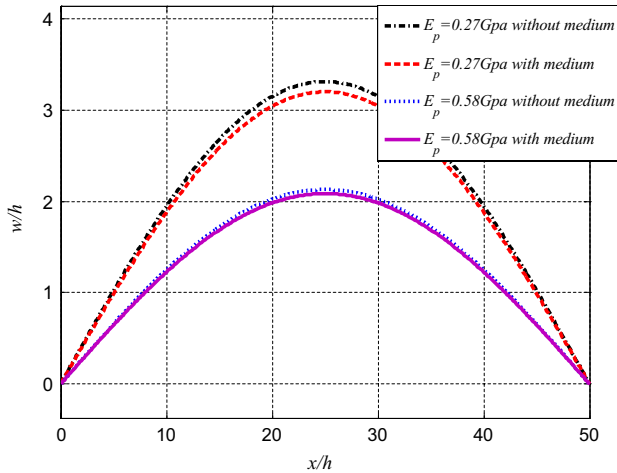

Fig. 7 The comparisons of dimensionless deflections for the CW theory versus the plastic modules concerning the effect of elastic medium

Fig. 8 The comparisons of the effective stresses versus the effective strain for the CW theory related two cases with medium and without it for two value of the normalized length scale

Fig. 9 The comparisons of dimensionless deflections versus the normalized variable length scale; l/h related two CW and MSG theories

Fig. 10 The comparison of the CW and MSG theories for the effective stress versus the effective strain ($l/h = 0.5$)

5 Solution Methodology

Due to complicated nonlinear terms in the total potential energy, the Rayleigh–Ritz method is implemented for calculating approximate solution. In this method, it is suitable to choose necessary functions satisfying geometrical boundary conditions. Then, by minimizing the functional of total potential energy in terms of the desirable displacements, one can obtain a homogeneous set of equations. In many problems of elastoplastic domains, the following simple base function is proposed for the simply-supported plate:

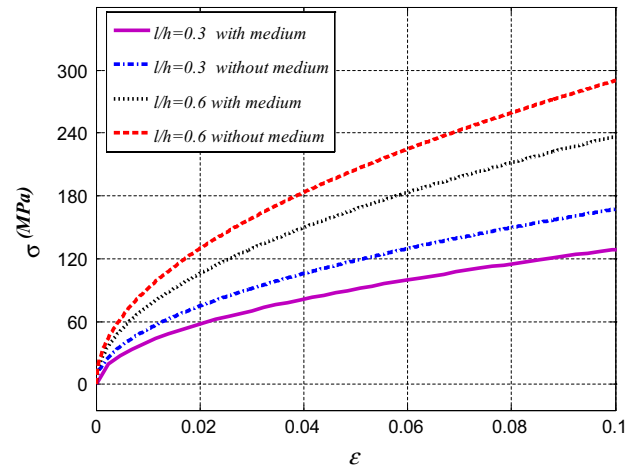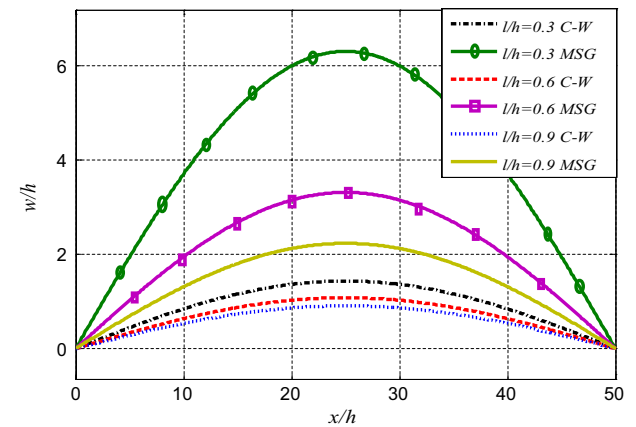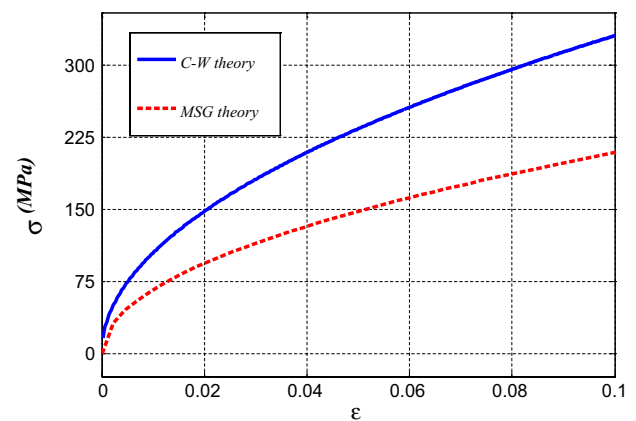$$w(x, y) = w sin\left(\frac{\pi}{a}x\right) sin\left(\frac{\pi}{b}y\right) \tag{57}$$

Eventually, we can obtain the displacement parameters by substituting relation (57) in the total potential energy and applying the Rayleigh–Ritz method: $\partial\Pi/\partial w = 0$.

6 Results and Discussions

At the previous section, we obtained the government relations for the plastic bending of microplate in two ways of MSG theory and CW hardening model. Now, the results of present study are introduced as well as comparison between two theories. Figure 3 shows that how vertical displacement may effect from the length scale for N = 0.2 by the MSG theory. Figures 4 illustrates the dimensionless deflections of the beam for the $l/h = 0.5$ versus the variable exponents of the plastic work hardening.

The comparisons of the effective stress for the MSG theory in terms of the effective strain are plotted in Fig. 5. The results include elastic medium for two value of the normalized length scale for N = 0.2.

According to the Ref. [33], the value of c_1 is so small due to being small amounts of the length scale as compared to the rotation gradient length scale so we considered it to $h/c_1 = 20$. In Fig. 6 the normalized deflections have been illustrated versus the normalized length scale for $E_p = 0.45$ Gpa with the Chen–Wang model. In Fig. 7, the normalized deflection is plotted versus the variable values of the tangency module; E_p and for this case we have $l/h = 0.5$. Curves in the Fig. 8 show the effect of length scale on stress for $E_p = 0.45$ Gpa. Also in all mentioned figures, the effect of medium is showed. These results are for $a/h = 10$ and $a/b = 1$ and $q/\sigma_Y hb = 0.001$. For the medium value of the parameter $K_w = 2.5$ MPa and $K_G = 5$ nN.

Corroding to the Figs. 3 and 6 in two model by increasing the length scale, vertical displacement is decreasing. In addition, the effect of length scale and medium on deflection in MSG theory is more significant. At the end, we present comparisons between two mentioned theories in Fig. 9 for normalized deflection and Fig. 10 for the effective stress–strain. Also,

$$E_p = \frac{d\sigma}{d\bar{\varepsilon}} = tan\theta = N\bar{\varepsilon}^{N-1} \tag{58}$$

For comparison of the critical force between two theories, we should consider the plastic work hardening exponent N = 1 and a plastic module for $\theta = 45$.

It is clear that the effect of length scale on deflection for the CW model is more tangible than the MSG model. These comparisons have been performed for $b/h = 10$, $a/b = 1$ and $q/\sigma_Y hb = 0.001$.

7 Conclusion

In this paper, plastic bending analysis of the microplates was predicted by using two Chen–Wang and Mechanism-Based strain gradient plasticity theories. The kinematics of the model was established on Kirchhoff formulation. Because of being many nonlinear terms in potential energy, analytical solution was impossible and we had to use Ritz method to obtain deflection. We showed the effect of length scale, work hardening exponent and plastic module on vertical displacement. Moreover, the influence of the Pasternak and Winkler foundations were regarded accounting for the elastic medium on deflection and stress fields.

For the similar geometry and material properties, we concluded that the MSG theory anticipated values of deflections of the micro plates more rather than the CW model. While the influence of material length scale in the CW theory was more important than MSG theory. In addition, the CW theory predicted the effective stress higher than the MSG. It is indicates that there is more tangible internal resistance for deflection.

The difference found in results is primarily due to the difference between CW theory and MSG/CMSG theory, not the difference between a lower-order theory and a higher-order SGP theory. In other words, the authors found similar differences between the lower-order CMSG and lower-order CW SGP.

This comparative study offer a simple benchmark model to examine permanent plastic behavior of the small size structures. These considerations can be developed in other aspects of the plasticity in metal forming process and plastic instability investigations that are interest of research in future.

References

1. C.S. Han, F. Roters, D. Raabe, Met. Mater. Int. **12**, 407–411 (2006)
2. L. Hu, S. Jiang, Y. Zhang, D. Sun, Met. Mater. Int. **23**, 1075–1086 (2017)
3. P. Maj, J. Zdunek, J. Mizera, K.J. Kurzydlowski, B. Sakowicz, M. Kaminski, Met. Mater. Int. **23**, 54–67 (2017)
4. B. Song, H. Zhao, L. Chai, N. Guo, H. Pan, H. Chen, R. Xin, Met. Mater. Int. **22**, 887–896 (2016)
5. A. Darvishvand, A. Zajkani, Microsyst. Technol. **25**, 4277–4289 (2019)
6. D. Kiener, C. Motz, T. Schöbert, M. Jenko, G. Dehm, Adv. Eng. Mater. **8**, 1119–1125 (2006)
7. J.S. Stölken, A.G. Evans, Acta Mater. **46**, 5109–5115 (1998)
8. S. Vakil, A. Zajkani, Mech. Mater. **137**, 103135 (2019)
9. N.A. Stelmashenko, M.G. Walls, L.M. Brown, Y.V. Milman, Acta Metall. Mater. **41**, 2855–2865 (1993)
10. N.A. Fleck, G.M. Muller, M.F. Ashby, J.W. Hutchinson, Acta Metall. Mater. **42**, 475–487 (1994)

11. A. Darvishvand, A. Zajkani, Meccanica (2019) (**accepted**)
12. C.W. Nan, D.R. Clarke, Acta Mater. **44**, 3801–3811 (1996)
13. A. Darvishvand, A. Zajkani, Eur. J. Mech. A/Solids **77**, 103777 (2019)
14. A. Darvishvand, A. Zajkani, Struct. Eng. Mech. Int. J. **71**, 223–232 (2019)
15. N. Huber, W.D. Nix, H. Gao, Proc. R. Soc. A Math. Phys. Eng. Sci. **458**, 1593–1620 (2002)
16. M.B. Taylor, H.M. Zbib, M.A. Khaleel, Int. J. Plast. **18**, 415–442 (2002)
17. I. Tsagrakis, E.C. Aifantis, Trans. ASME **124**, 352–357 (2002)
18. W.D. Nix, H. Gao, J. Mech. Phys. Solids **46**, 411–425 (1998)
19. P. Cermelli, M.E. Gurtin, Int. J. Solids Struct. **39**, 6281–6309 (2002)
20. L.P. Evers, W.A.M. Brekelmans, M.G.D. Geers, Int. J. Solids Struct. **41**, 5209–5230 (2004)
21. M.G.D. Geers, W.A.M. Brekelmans, C.J. Bayley, Model. Simul. Mater. Sci. Eng., 15(1), S133–S145 (2007)
22. A. Acharya, A.J. Beaudoin, J. Mech. Phys. Solids **48**, 2213–2230 (2000)
23. H. Gao, Y. Huang, W.D. Nix, J.W. Hutchinson, J. Mech. Phys. Solids **47**, 1239–1263 (1999)
24. Y. Huang, H. Gao, W.D. Nix, J.W. Hutchinson, J. Mech. Phys. Solids **48**, 99–128 (2000)
25. Y. Huang, S. Qu, K.C. Hwang, M. Li, H. Gao, Int. J. Plast. **20**, 753–782 (2004)
26. S.H. Chen, T.C. Wang, Acta Mater. **48**, 3997–4005 (2000)
27. H.B. Muhlhaus, E.C. Aifantis, Acta Mech. **89**, 217–231 (1991)
28. N.A. Fleck, J.W. Hutchinson, J. Mech. Phys. Solids **41**, 1825–1857 (1993)
29. N.A. Fleck, J.W. Hutchinson, Adv. Appl. Mech. **33**, 295–361 (1997)
30. N.A. Fleck, J.W. Hutchinson, J. Mech. Phys. Solids **49**, 2245–2271 (2001)
31. P. Gudmundson, J. Mech. Phys. Solids **52**, 1379–1406 (2004)
32. S.K. Park, X.-L. Gao, J. Micromech. Microeng. **16**, 2355–2359 (2006)
33. S.H. Chen, B. Feng, Acta Mech. **219**, 291–307 (2011)
34. N. Challamel, C.M. Wang, Nanotechnology **19**, 1–7 (2008)
35. W. Wang, Y. Huang, K.J. Hsia, K.X. Hu, A. Chandra, Int. J. Plast. **19**, 365–382 (2003)
36. B.N. Patel, D. Pandit, S.M. Srinivasan, Procedia Eng. **173**, 1064–1070 (2017)
37. Y.Q. Mao, S.G. Ai, D.N. Fang, Y.M. Fu, C.P. Chen, Compos. Struct. **101**, 168–179 (2013)
38. Z.F. Shi, B. Huang, H. Tan, Y. Huang, T.Y. Zhang, P.D. Wu, K.C. Hwang, H. Gao, Int. J. Plast. **24**, 1606–1624 (2008)
39. A. Arsenlis, D.M. Parks, Acta Mater. **47**, 1597–1611 (1999)
40. S.H. Chen, T.C. Wang, Int. J. Plast. **18**, 971–995 (2002)
41. H. Ban, Y. Yao, S. Chen, D. Fang, Int. J. Plast. **95**, 251–263 (2017)
42. H. Ban, Y. Yao, S. Chen, D. Fang, Int. J. Mech. Sci. **152**, 524–534 (2019)
43. K.A. Lazopoulos, Mech. Res. Commun. **36**, 777–783 (2009)
44. W.Y. Jung, W.T. Park, S.C. Han, Int. J. Mech. Sci. **87**, 150–162 (2014)
45. B. Zhang, Y. He, D. Liu, L. Shen, J. Lei, Appl. Math. Model. **39**, 3814–3845 (2015)
46. K.M. Liew, X.Q. He, S. Kitipornchai, Acta Mater. **54**, 4229–4236 (2006)
47. D.A. Dillard, B. Mukherjee, P. Karnal, R.C. Batra, J. Frechette, Soft Matter **14**, 3669–3683 (2018)
48. X. You, J.J. Pak, in *2013 Transducers Eurosensors XXVII 17th International Conference Solid-State Sensors, Actuators Microsystems, Transducers Eurosensors 2013*, pp. 2443–2446 (2013)
49. J.F.W. Bishop, R. Hill, Lond. Edinb. Dublin Philos. Mag. J. Sci. **42**, 1298–1307 (1951)
50. J.F.W. Bishop, R. Hill, Philos. Mag. Ser. **7**(42), 414–427 (1951)
51. L. Zhou, S. Li, S. Huang, Mater. Des. **32**, 353–360 (2011)
52. A. Darvishvand, A. Zajkani, Mech. Based Des. Struct. Mach. (2019). https://doi.org/10.1080/15397734.2019.1705167
53. A. Zajkani, A. Darvizeh, M. Darvizeh, R. Ansari, J. Strain Anal. Eng. Des. **49**, 86–111 (2014)